

A&A 521, L9 (2010)
DOI: [10.1051/0004-6361/201014959](https://doi.org/10.1051/0004-6361/201014959)
© ESO 2010

**Astronomy
&
Astrophysics**
Special feature

Herschel/HIFI: first science highlights

LETTER TO THE EDITOR

Herschel/HIFI discovery of interstellar chloronium (H_2Cl^+)^{*,**}

D. C. Lis¹, J. C. Pearson¹³, D. A. Neufeld³, P. Schilke^{8,12}, H. S. P. Müller¹², H. Gupta¹³, T. A. Bell¹, C. Comito⁸, T. G. Phillips¹, E. A. Bergin², C. Ceccarelli⁶, P. F. Goldsmith¹³, G. A. Blake¹, A. Bacmann^{6,23}, A. Baudry²³, M. Benedettini²⁴, A. Benz³⁷, J. Black³⁶, A. Boogert¹⁶, S. Bottinelli^{4,5}, S. Cabrit²⁵, P. Caselli²⁶, A. Castets⁶, E. Caux^{4,5}, J. Cernicharo⁷, C. Codella²⁷, A. Coutens^{4,5}, N. Crimier^{6,7}, N. R. Crockett², F. Daniel^{7,9}, K. Demyk^{4,5}, C. Dominic^{28,29}, M.-L. Dubernet^{10,11}, M. Emprechtinger¹, P. Encrenaz²⁵, E. Falgarone⁹, A. Fuente³⁰, M. Gerin⁹, T. F. Giesen¹², J. R. Goicoechea⁷, F. Helmich²⁰, P. Hennebelle⁹, Th. Henning⁴⁵, E. Herbst¹⁴, P. Hily-Blant⁶, Å. Hjalmarsen³⁸, D. Hollenbach³⁹, T. Jack²³, C. Joblin^{4,5}, D. Johnstone¹⁵, C. Kahane⁶, M. Kama²⁸, M. Kaufman⁴⁰, A. Klotz^{4,5}, W. D. Langer¹³, B. Larsson⁴¹, J. Le Bourlot⁴², B. Lefloch⁶, F. Le Petit⁴², D. Li¹³, R. Liseau³⁶, S. D. Lord¹⁶, A. Lorenzani²⁴, S. Maret⁶, P. G. Martin¹⁷, G. J. Melnick¹⁸, K. M. Menten⁸, P. Morris¹³, J. A. Murphy¹⁹, Z. Nagy²¹, B. Nisini³¹, V. Ossenkopf^{12,20}, S. Pacheco⁶, L. Pagani²⁵, B. Parise⁸, M. Péroult⁹, R. Plume²¹, S.-L. Qin¹², E. Roueff⁴², M. Salez^{25,44}, A. Sandqvist⁴³, P. Saraceno³², S. Schlemmer¹², K. Schuster³³, R. Snell²², J. Stutzki¹², A. Tielens³⁴, N. Trappe¹⁹, F. F. S. van der Tak^{21,46}, M. H. D. van der Wiel^{21,46}, E. van Dishoeck³⁴, C. Vastel^{4,5}, S. Viti³⁵, V. Wakelam²³, A. Walters^{4,5}, S. Wang², F. Wyrowski⁸, H. W. Yorke¹³, S. Yu¹³, J. Zmuidzinas¹, Y. Delorme⁴⁴, J.-P. Desbat²³, R. Güsten⁸, J.-M. Krieg⁴⁴, and B. Delforge⁴⁴

(Affiliations are available on page 5 of the online edition)

Received 9 May 2010 / Accepted 14 June 2010

ABSTRACT

We report the first detection of chloronium, H_2Cl^+ , in the interstellar medium, using the HIFI instrument aboard the *Herschel* Space Observatory. The $2_{12}-1_{01}$ lines of ortho- $\text{H}_2^{35}\text{Cl}^+$ and ortho- $\text{H}_2^{37}\text{Cl}^+$ are detected in absorption towards NGC 6334I, and the $1_{11}-0_{00}$ transition of para- $\text{H}_2^{35}\text{Cl}^+$ is detected in absorption towards NGC 6334I and Sgr B2(S). The H_2Cl^+ column densities are compared to those of the chemically-related species HCl. The derived HCl/ H_2Cl^+ column density ratios, $\sim 1-10$, are within the range predicted by models of diffuse and dense photon dominated regions (PDRs). However, the observed H_2Cl^+ column densities, in excess of 10^{13} cm^{-2} , are significantly higher than the model predictions. Our observations demonstrate the outstanding spectroscopic capabilities of HIFI for detecting new interstellar molecules and providing key constraints for astrochemical models.

Key words. astrochemistry – line: identification – ISM: abundances – ISM: molecules – molecular processes – submillimetre: ISM

1. Introduction

The halogen elements, fluorine and chlorine, form hydrides that are very strongly bound: hydrogen fluoride is the only diatomic hydride, and HCl^+ the only diatomic hydride cation, with a dissociation energy exceeding that of molecular hydrogen. Drawing upon earlier work by Jura (1974), Dalgarno et al. (1974), van Dishoeck & Black (1986), Blake et al. (1986), Schilke et al. (1995), Federman et al. (1995), and Amin (1996), Neufeld & Wolfire (2009; hereafter NW09) have recently carried out a theoretical study of the chemistry of chlorine-bearing molecules, in both diffuse and dense molecular clouds. In diffuse interstellar gas clouds, the dominant ionization state of every element is determined by its ionization potential. Chlorine, with an ionization potential slightly lower than that of hydrogen, is predominantly singly-ionized. The Cl^+ ion can react exothermically

with H_2 , the dominant molecular constituent of the interstellar medium (ISM):



The product of this reaction is the reactive HCl^+ ion, which undergoes further reaction with H_2 to form H_2Cl^+ :



The H_2Cl^+ molecule does not react with H_2 , and is destroyed by dissociative recombination and proton transfer to CO, both of which are sources of hydrogen chloride, HCl.

Prior to the launch of *Herschel*, the H^{35}Cl and H^{37}Cl isotopologues were the only chlorine-containing molecules to have been detected in the ISM (e.g., Blake et al. 1985; Zmuidzinas et al. 1995; Schilke et al. 1995; Salez et al. 1996; see also recent HIFI observations of Cernicharo et al. 2010)¹. However, predictions for the chemistry of Cl-bearing interstellar molecules

* *Herschel* is an ESA space observatory with science instruments provided by European-led Principal Investigator consortia and with important participation from NASA.

** Table 1 and acknowledgments (page 5) are only available in electronic form at <http://www.aanda.org>

¹ The metal halides NaCl, KCl, and AlCl have been detected in the *circumstellar envelope* of the evolved star IRC+10216, with abundances that reflect the thermochemical equilibrium established within the stellar photosphere (Cernicharo & Guélin 1987).

(NW09) have identified chloronium, H_2Cl^+ , as a relatively abundant species that is potentially detectable. H_2Cl^+ is predicted to be most abundant in those environments where the ultraviolet radiation is strong: in diffuse clouds, or near the surfaces of dense clouds that are illuminated by nearby O and B stars. In such environments, the photoionization of atomic chlorine leads to a large abundance of Cl^+ ions that can form HCl^+ and H_2Cl^+ through reactions (1) and (2). A secondary abundance peak occurs in dense, shielded regions; here HCl becomes a significant reservoir of gas-phase chlorine, and can produce H_2Cl^+ through reaction with H_3^+ :



However, the chlorine depletion is typically large within such regions (Schilke et al. 1995) and thus the overall H_2Cl^+ abundance is rather small.

In diffuse molecular clouds of density $n_{\text{H}} = 10^{2.5} \text{ cm}^{-3}$, H_2 column density $\geq 10^{20} \text{ cm}^{-2}$, and χ_{UV} in the range 1–10 (where χ_{UV} is the UV radiation field normalized with respect to the mean interstellar value, Draine 1978), the NW09 model predicts H_2Cl^+ column densities $\sim 3 \times 10^{10} \chi_{\text{UV}} \text{ cm}^{-2}$. In dense PDRs ($n_{\text{H}} = 10^4 \text{ cm}^{-3}$) illuminated by strong radiation fields ($\chi_{\text{UV}} > 10^3$), the predicted H_2Cl^+ column densities are $\sim 10^{12} \text{ cm}^{-2}$.

In this Letter, we report the first detection of chloronium towards NGC 6334I and Sgr B2(S), obtained using the HIFI instrument (de Graauw et al. 2010) aboard the *Herschel* Space Observatory (Pilbratt et al. 2010). NGC 6334 is a luminous and relatively nearby (1.7 kpc) molecular cloud/H II region complex containing several concentrations of massive stars at various stages of evolution. The far-infrared source “I”, located at the northeastern end of the complex, is associated with a NIR cluster of bolometric luminosity of $2.6 \times 10^5 L_{\odot}$ (Sandell 2000), with four embedded compact millimeter continuum sources (Hunter et al. 2006). Sgr B2(S) is a strong submillimeter continuum source with a much less complex hot core emission spectrum, as compared to its better known neighbor Sgr B2(M). This makes it a prime candidate for absorption studies, probing the entire sight-line between the Sun and the Galactic center, with clouds in the Orion, Sagittarius, and Scutum spiral arms easily identified at separate velocities (e.g., Greaves & Nyman 1996).

2. Observations

HIFI observations presented here were carried out between 2010 March 1 and March 23, using the dual beam switch (DBS) observing mode, as part of guaranteed and open time key programs CHESS: Chemical *Herschel* Spectral Surveys, HEXOS: *Herschel*/HIFI observations of EXtra-Ordinary Sources: The Orion and Sagittarius B2 starforming regions, and HOP: *Herschel* oxygen program. The source coordinates are: $\alpha_{J2000} = 17^{\text{h}}20^{\text{m}}53.32^{\text{s}}$ and $\delta_{J2000} = -35^{\circ}46'58.5''$ for NGC 6334I, and $\alpha_{J2000} = 17^{\text{h}}47^{\text{m}}20.3^{\text{s}}$ and $\delta_{J2000} = -28^{\circ}23'43.0''$ for Sgr B2(S). The DBS reference beams lie approximately $3'$ east and west (i.e. perpendicular to the roughly north-south elongation of the two sources). Because the DBS mode alternates between two reference positions, separated by $6'$ on the sky, we used the Level 1 data to compute a difference spectrum between the two reference positions to check for possible contamination in the reference beams; we see no evidence for emission or absorption in such a difference spectrum. We used the HIFI wide band spectrometer (WBS) providing a spectral resolution of 1.1 MHz ($\sim 0.4 \text{ km s}^{-1}$ at 780 GHz) over a 4 GHz IF bandwidth. The spectra presented here are averages of the H and V polarizations, with equal weighting, reduced using HIPE (Ott 2010) with pipeline

version 2.6. The resulting Level 2 DSB spectra were exported to the FITS format for a subsequent data reduction and analysis using the IRAM GILDAS package (<http://iram.fr/IRAMFR/GILDAS>).

The band 2b, 1b and 1a spectral scans of NGC 6334I consist of double sideband spectra (DSB) with a redundancy of 8, which gives observations of a lower or upper sideband frequency with 8 different settings of the local oscillator (LO). The Sgr B2(S) data consist of 8 LO settings with a high redundancy of 12, centered near the frequency of the 487.2 GHz line of O_2 . The observations were fine-tuned so that 4 of the 8 LO settings cover the frequency of the p- H_2Cl^+ line. These observing modes allow for the deconvolution and isolation of a single sideband spectrum (Comito & Schilke 2002). We applied the standard deconvolution routine within CLASS. All NGC 6334I data presented here are deconvolved single sideband spectra, including the continuum. The HCl data in Sgr B2(S) were obtained using the DBS single point observing mode with 3 shifted LO settings that were averaged to produce the final spectrum. The HIFI beam size at 485 GHz and 780 GHz is $44''$ and $30''$, respectively, with main beam efficiency of ~ 0.68 .

3. Spectroscopy of H_2Cl^+

The H_2Cl^+ ion is a closed-shell molecule, isoelectronic with H_2S . Like H_2S and water, H_2Cl^+ is a highly asymmetric top, exhibiting a b-type rotational spectrum. Its fairly large dipole moment, calculated ab initio to be 1.89 D (Müller et al. 2005), about 70% larger than that of HCl (1.109 D; de Leluw & Dymanus 1973), results in strong lines in the THz range. Araki et al. (2001) measured rotational spectra of $\text{H}_2^{35}\text{Cl}^+$, $\text{H}_2^{37}\text{Cl}^+$, and HDCl^+ below 500 GHz. The accurate spectroscopic constants derived from these measurements, including electric quadrupole coupling parameters, yield a central bond angle in H_2Cl^+ of $\sim 94.2^\circ$ (similar to that of H_2S , 92.2° ; Burrus & Gordy 1953), and permit the prediction of the ground state ortho transitions of H_2Cl^+ and $\text{H}_2^{37}\text{Cl}^+$ near 780 GHz to well within 1 MHz (see Table 1).

4. Results

4.1. NGC 6334I

Strong absorption at the frequency of the $2_{12}-1_{01}$ transition of o- $\text{H}_2^{35}\text{Cl}^+$ at 781.6 GHz in NGC 6334I (Fig. 1a) has provided the initial identification. Fitting the o- $\text{H}_2^{35}\text{Cl}^+$ $2_{12}-1_{01}$ hyperfine structure (HFS) gives a line velocity of -1.7 km s^{-1} for the strongest hyperfine component and a line width of 11.6 km s^{-1} . The OH absorption profiles (Brooks & Whiteoak 2001) reveal two molecular clouds located along the line of sight to NGC 6334, one with velocities extending from -15 to 2 km s^{-1} , and one with a well-defined velocity near 6 km s^{-1} . The hot core emission lines peak at about -6.5 km s^{-1} (e.g., C^{18}O 7–6 in the same band; HCl , Sect. 4.1). Water and CH spectra towards NGC 6334I show multiple velocity components, including absorption near 0 km s^{-1} , close to the $\text{H}_2^{35}\text{Cl}^+$ velocity (Emprechtinger et al. 2010; van der Wiel et al. 2010). The chloronium line velocity in NGC 6334I is in good agreement with the H_2O^+ absorption velocity, also a tracer of diffuse gas, when H_2O^+ frequencies of Mürtz et al. (1998) are used (see Schilke et al. 2010 for a discussion of the H_2O^+ line frequencies). The large H_2Cl^+ line width may be due to blending of multiple absorption components. However, the H_2O^+ line width is also quite large, about 8 km s^{-1} .

The corresponding line of o- $\text{H}_2^{37}\text{Cl}^+$ is also detected (Fig. 1b). However, the spectrum is contaminated by interfering emission of dimethyl ether (light-blue line in Fig. 1b), one of

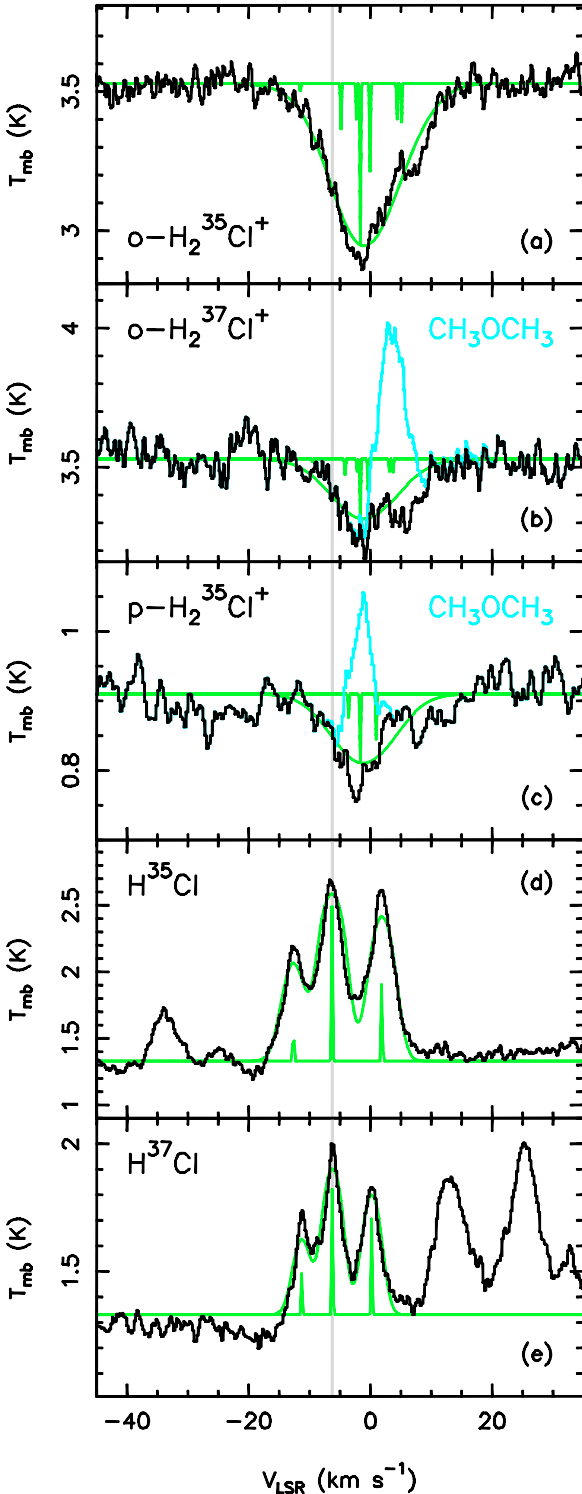


Fig. 1. Spectra of chlorine species in NGC 6334I: **a)** o- $\text{H}_2^{35}\text{Cl}^+$ $2_{12}-1_{01}$; **b)** o- $\text{H}_2^{37}\text{Cl}^+$ $2_{12}-1_{01}$; **c)** p- $\text{H}_2^{35}\text{Cl}^+$ $1_{11}-0_{00}$; **d)** H^{35}Cl $1-0$; and **e)** H^{37}Cl $1-0$. The velocity scale corresponds to the strongest HFS components. Green lines show HFS fits and positions of the HFS components. The o- $\text{H}_2^{37}\text{Cl}^+$ and p- $\text{H}_2^{35}\text{Cl}^+$ lines are blended with dimethyl ether emission (light-blue lines in panels **b)** and **c)**).

the most abundant “weeds” in NGC 6334I. The contamination is subtracted by using an LTE model that fits profiles of nearby dimethyl ether lines with similar upper level energies (Endres et al. 2009). The resulting o- $\text{H}_2^{37}\text{Cl}^+$ spectrum is shown as a black line in Fig. 1b. The $1_{11}-0_{00}$ line of p- $\text{H}_2^{35}\text{Cl}^+$ (Fig. 1c) is also blended with dimethyl ether emission, similarly subtracted.

H_2Cl^+ spectra in NGC 6334I can be compared to those of the chemically related species HCl (Fig. 1d and 1e). The lines of H^{35}Cl and H^{37}Cl are detected in emission at the hot core velocity ($\sim -6.3 \text{ km s}^{-1}$), with narrow line widths of 4.1 and 3.3 km s^{-1} , respectively. The HCl HFS is resolved spectrally using HIFI WBS, allowing for the determination of the line opacity.

We have modelled the H_2Cl^+ spectra assuming the same excitation temperature of 5 K for all hyperfine components². A low value of the excitation temperature is justified given the high spontaneous emission rates and critical densities of the transitions considered here and it provides a lower limit for the molecular column densities derived from absorption measurements. An HFS fit to the $2_{12}-1_{01}$ transition of o- $\text{H}_2^{35}\text{Cl}^+$ (green line in Fig. 1a) gives an o- $\text{H}_2^{35}\text{Cl}^+$ column density of $1.3 \times 10^{13} \text{ cm}^{-2}$, under the assumption that the absorption completely covers the continuum and is not concentrated in small clumps. A fit to the $1_{11}-0_{00}$ spectrum of p- $\text{H}_2^{35}\text{Cl}^+$, with all parameters other than the column density fixed, gives a p- $\text{H}_2^{35}\text{Cl}^+$ column density of $4.0 \times 10^{12} \text{ cm}^{-2}$. The total $\text{H}_2^{35}\text{Cl}^+$ column density is thus $1.7 \times 10^{13} \text{ cm}^{-2}$ and the ortho-to-para ratio is 3.2, consistent with the statistical weight ratio. For an excitation temperature of 2.7 K, the ortho and para H_2Cl^+ column densities are approximately 10% and 20% lower, respectively. The $\text{H}_2^{35}\text{Cl}^+$ spectra are all optically thin (line center optical depth of ~ 0.2 for the ortho line). We derive an $\text{H}_2^{35}\text{Cl}^+/\text{H}_2^{37}\text{Cl}^+$ ratio of 3, close to the terrestrial ratio of 3.1.

We have modelled the H^{35}Cl and H^{37}Cl emission spectra assuming a source size of $10''$ (approximate size of the cluster of compact continuum sources seen in the SMA image of Hunter et al. 2006). Under this assumption, a least squares fit to the H^{35}Cl spectrum gives an excitation temperature of 31 K and a column density of $4.0 \times 10^{14} \text{ cm}^{-2}$. For H^{37}Cl , we derive an excitation temperature of 21 K and a column density of $1.5 \times 10^{14} \text{ cm}^{-2}$; the resulting $\text{H}^{35}\text{Cl}/\text{H}^{37}\text{Cl}$ ratio is 2.7. However, HCl column densities and the isotopic ratio depend strongly on the assumed source size (for a source size of $5''$ the derived isotopic ratio is 4.1). The $350 \mu\text{m}$ continuum flux density toward NGC 6334I is 1430 Jy in a $9''$ beam (CSO/SHARC II; Dowell et al., private comm.) Assuming a dust temperature of 100 K (Sandell 2000) and a grain emissivity $\kappa_{350} = 0.1 \text{ cm}^2 \text{ g}^{-1}$, we derive an H_2 column density of $1.2 \times 10^{24} \text{ cm}^{-2}$, which implies an H^{35}Cl abundance of $\sim 1.7 \times 10^{-10}$ with respect to H nuclei. The lines of both HCl isotopologues are optically thick, with line center optical depths of ~ 2.2 and 1.6 for the strongest hyperfine component of H^{35}Cl and H^{37}Cl , respectively.

4.2. Sgr B2(S)

The p- $\text{H}_2^{35}\text{Cl}^+$ spectrum towards Sgr B2(S) (Fig. 2, upper panel) shows strong absorption near the systemic velocity of the Sgr B2 envelope ($\sim 62 \text{ km s}^{-1}$) and two additional deep absorption components between 0 and 20 km s^{-1} . In addition, shallow absorption is seen over a broad range of velocities down to -100 km s^{-1} , in agreement with the HI absorption spectrum towards the nearby source Sgr B2(M) (magenta line in Fig. 2). Both H^{35}Cl and H^{37}Cl (Fig. 2, lower panel) show deep absorption at the envelope velocity and a shallow absorption between 0

² We made use of the myXCLASS program (<http://www.astro.uni-koeln.de/projects/schilke/XCLASS>), which accesses the CDMS (Müller et al. 2001; Müller et al. 2005; <http://www.cdms.de>) and JPL (Pickett et al. 1998; <http://spec.jpl.nasa.gov>) molecular databases.

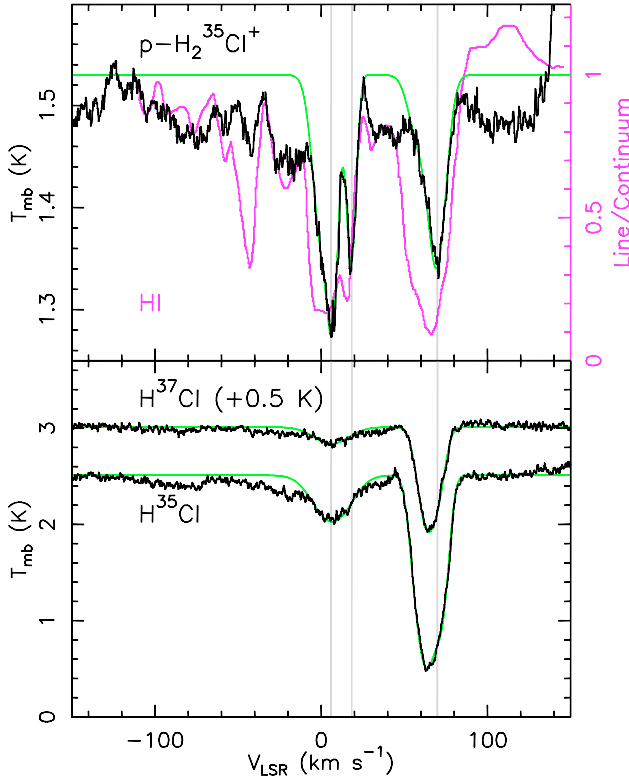


Fig. 2. Spectra of $p\text{-H}_2^{35}\text{Cl}^+ 1_{11}-0_{00}$ (upper panel), and H^{35}Cl and H^{37}Cl $1-0$ (lower panel) towards Sgr B2(S). The H^{37}Cl spectrum has been shifted up by 0.5 K. The magenta line in the upper panel shows the H I absorption spectrum towards Sgr B2(M) (from Garwood & Dickey 1989).

and 20 km s^{-1} . Similarly to NGC 6334I, we see velocity offsets of order a few km s^{-1} between HCl and H_2Cl^+ components.

Assuming a 5 K excitation temperature (the same as for NGC 6334I) and an ortho/para ratio of 3, we derive H_2Cl^+ column densities of 3.4×10^{13} and $2.2 \times 10^{13} \text{ cm}^{-2}$ for the 0 and 62 km s^{-1} components, with corresponding H^{35}Cl column densities of 4×10^{13} and $2 \times 10^{14} \text{ cm}^{-2}$. The $\text{H}^{35}\text{Cl}/\text{H}^{37}\text{Cl}$ ratio is ~ 3.3 in both components. We estimate the uncertainties in our molecular column density estimates to be of order a factor of 2.

To derive the hydrogen column density in the foreground gas towards Sgr B2(S), we use the method employed in Lis et al. (2001) to analyze the O I absorption towards Sgr B2(M), based on H I and ^{13}CO absorption data. We assume that the foreground absorption is extended and column densities are the same towards Sgr B2(M) and (S). We derive a total hydrogen nuclei column density of $\sim 2 \times 10^{22} \text{ cm}^{-2}$ in the atomic and molecular components in the velocity range -10 to 20 km s^{-1} (with a factor of 2 uncertainty). The corresponding chlorine content, in the form of H_2Cl^+ and HCl, is $7 \times 10^{13} \text{ cm}^{-2}$, implying a Cl/H ratio of $\sim 4 \times 10^{-9}$. This can be compared to the values measured in the UV in diffuse clouds (e.g., Sonnentrucker et al. 2006), which are in the range 3×10^{-8} – 4×10^{-7} . Therefore the high H_2Cl^+ column densities we derive here are consistent with the overall chlorine budget, leaving plenty of room for atomic Cl and depletion on dust grains.

5. Discussion

Our estimates of the H_2Cl^+ column densities towards NGC 6334I and Sgr B2(S), in excess of 10^{13} cm^{-2} , are significantly higher than those expected for a single dense or diffuse PDR viewed at normal incidence. This might point to some

deficiency in the models. Alternatively, a significant enhancement in the absorbing column density could result if the normal to the irradiated surface were inclined relative to the sight-line, or indeed if multiple PDRs were present along the sight-line, particularly if the radiation field is enhanced, as may be likely for the multiple absorption components seen towards Sgr B2. Similar discrepancies between models and observations are seen for other reactive ions in massive starforming regions (e.g., CO^+ toward AFGL 2591; Bruderer et al. 2009).

We derive an $\text{HCl}/\text{H}_2\text{Cl}^+$ ratio of ~ 10 in NGC 6334I and the Sgr B2 envelope (assuming that in the case of NGC 6334I the H_2Cl^+ column density on the back side is the same as that derived in front of the continuum source from our absorption measurements). This is well within the range predicted for dense PDRs (up to ~ 100 for densities above 10^6 cm^{-3}). The $\text{HCl}/\text{H}_2\text{Cl}^+$ ratio derived in the foreground gas towards Sgr B2(S) at velocities 0 – 20 km s^{-1} , ~ 1 , is also consistent with predictions of diffuse cloud models.

While a detailed analysis of chlorine chemistry in these and other sources that have been or will be observed using HIFI will be presented in a forthcoming paper, this work clearly demonstrates the outstanding spectroscopic capabilities of HIFI in the search for new interstellar molecules, particularly hydrides, and in providing robust constraints for astrochemical models of the interstellar medium.

References

- Amin, M. Y. 1996, EMP, 73, 133
- Araki, M., Furuya, T., & Saito, S. 2001, J. Mol. Spec., 210, 132
- Blake, G. A., Keene, J., & Phillips, T. G. 1985, ApJ, 295, 501
- Blake, G. A., Anacich, V. G., & Huntress, W. T. 1986, ApJ, 300, 415
- Brooks, K. J., & Whiteoak, J. B. 2001, MNRAS, 320, 465
- Bruderer, S., Benz, A. O., Doty, S. D., et al. 2009, ApJ, 700, 872
- Burrus, Jr., C. A., Daniel, F., & Gordy, W. 1953, Phys. Rev., 92, 274
- Cernicharo, J., & Guélin, M. 1987, A&A, 183, L10
- Cernicharo, J., Goicoechea, J. R., Daniel, F., et al. 2010, A&A, 518, L115
- Comito, C., & Schilke, P. 2002, A&A, 395, 357
- Dalgarno, A., de Jong, T., Oppenheimer, M., & Black, J. 1974, ApJ, 192, L37
- de Graauw, Th., Helmich F. P., Phillips, T. G., et al. 2010, A&A, 518, L6
- de Leluw, F. H., & Dymanus, A. 1973, J. Mol. Spec., 48, 427
- Draine, B. T. 1978, ApJS, 36, 595
- Emprechtinger, M., Lis, D. C., Bell, T., et al. 2010, A&A, 521, L28
- Endres, C. P., Drouin, B. J., Pearson, J. C., et al. 2009, A&A, 504, 635
- Federman, S. R., Cardell, Jason A., van Dishoeck, E. F., et al. 1995, ApJ, 445, 325
- Garwood, R. W., & Dickey, J. M. 1989, ApJ, 338, 841
- Greaves, J. S., & Nyman, L.-A. 1996, A&A, 305, 950
- Hunter, T. R., Brogan, C. L., Megeath, S. T., et al. 2006, ApJ, 649, 888
- Jura, M. 1974, ApJ, 190, L33
- Lis, D. C., Keene, J., Phillips, T. G., et al. 2001, ApJ, 561, 823
- Müller, H. S. P., Thorwirth, S., Roth, D. A., & Winnewisser, G. 2001, A&A, 370, L49
- Müller, H. S. P., Schlöder, F., Stutzki, J., & Winnewisser, G. 2005, J. Mol. Struct., 742, 215
- Mürtz, P., Zink, L. R., Evenson, K. M., & Brown, J. M. 1998, J. Chem. Phys., 109, 9744
- Neufeld, D. A., & Wolfire, M. G. 2009, ApJ, 706, 1594 (NW09)
- Ott, S. 2010, in Astronomical Data Analysis Software and Systems XIX, ed. Y. Mizumoto, K.-I. Morita, & M. Ohishi, ASP Conf. Ser., in press
- Pickett, H. M., Poynter, R. L., Cohen, E. A., et al. 1998, J. Quant. Spectrosc. Radiat. Transf., 60, 883
- Pilbratt, G. L., Riedinger, J. R., Passvogel, T., et al. 2010, A&A, 518, L1
- Salez, M., Frerking, M. A., & Langer, W. D. 1996, ApJ, 467, 708
- Sandell, G. 2000, A&A, 358, 242
- Schilke, P., Phillips, T. G., & Wang, N. 1995, ApJ, 441, 334
- Schilke, P., Comito, C., Müller, H. S. P., et al. 2010, A&A, 521, L11
- Sonnentrucker, P., Friedman, S. D., & York, D. G. 2006, ApJ, 650, L115
- van der Wiel, M. H. D., van der Tak, F. F. S., Lis, D. C., et al. 2010, A&A, 521, L43
- van Dishoeck, E. F., & Black, J. H. 1986, ApJS, 62, 109
- Zmuidzinas, J., Blake, G. A., Carlstrom, J., et al. 1995, ApJ, 447, L125

Table 1. Frequencies of the H_2Cl^+ transitions observed.

Transition	Frequency (MHz)	Error (MHz)	A_{ij} (s^{-1})	E_l (cm^{-1})
$\text{H}_2^{35}\text{Cl}^+$				
$1_{11}-0_{00} \ 3/2-3/2$	485413.427	0.029	0.00159	0
$5/2-3/2$	485417.670	0.015	0.00159	0
$1/2-3/2$	485420.796	0.057	0.00159	0
$2_{12}-1_{01} \ 5/2-5/2$	781609.303	0.063	0.00179	14.1
$3/2-1/2$	781611.062	0.062	0.00248	14.1
$5/2-3/2$	781622.721	0.063	0.00417	14.1
$7/2-5/2$	781626.794	0.060	0.00596	14.1
$1/2-1/2$	781628.554	0.061	0.00496	14.1
$3/2-3/2$	781635.214	0.062	0.00318	14.1
$\text{H}_2^{37}\text{Cl}^+$				
$2_{12}-1_{01} \ 5/2-5/2$	780037.315	0.069	0.00178	14.1
$3/2-1/2$	780038.760	0.066	0.00247	14.1
$5/2-3/2$	780047.903	0.066	0.00414	14.1
$7/2-5/2$	780051.197	0.062	0.00592	14.1
$1/2-1/2$	780052.642	0.065	0.00493	14.1
$3/2-3/2$	780057.820	0.068	0.00316	14.1

Notes. Frequencies and spontaneous emission coefficients have been calculated from the constants derived by Araki et al. (2001), see also CDMS.

Acknowledgements. HIFI has been designed and built by a consortium of institutes and university departments from across Europe, Canada and the United States under the leadership of SRON Netherlands Institute for Space Research, Groningen, The Netherlands and with major contributions from Germany, France and the US. Consortium members are: Canada: CSA, U. Waterloo; France: CESR, LAB, LERMA, IRAM; Germany: KOSMA, MPIfR, MPS; Ireland, NUI Maynooth; Italy: ASI, IFSI-INAF, Osservatorio Astrofisico di Arcetri-INAF; Netherlands: SRON, TUD; Poland: CAMK, CBK; Spain: Observatorio Astronómico Nacional (IGN), Centro de Astrobiología (CSIC-INTA). Sweden: Chalmers University of Technology – MC2, RSS & GARD; Onsala Space Observatory; Swedish National Space Board, Stockholm University – Stockholm Observatory; Switzerland: ETH Zurich, FHNW; USA: Caltech, JPL, NHSC. Support for this work was provided by NASA through an award issued by JPL/Caltech. D. C. L. is supported by the NSF, award AST-0540882 to the CSO. A portion of this research was performed at the Jet Propulsion Laboratory, California Institute of Technology, under contract with the National Aeronautics and Space Administration.

- ¹ California Institute of Technology, Cahill Center for Astronomy and Astrophysics 301-17, Pasadena, CA 91125, USA
e-mail: dcl@caltech.edu
- ² Department of Astronomy, University of Michigan, 500 Church Street, Ann Arbor, MI 48109, USA
- ³ Department of Physics and Astronomy, Johns Hopkins University, 3400 North Charles Street, Baltimore, MD 21218, USA
- ⁴ Centre d'Étude Spatiale des Rayonnements, Université de Toulouse [UPS], 31062 Toulouse Cedex 9, France
- ⁵ CNRS/INSU, UMR 5187, 9 avenue du Colonel Roche, 31028 Toulouse Cedex 4, France
- ⁶ Laboratoire d'Astrophysique de l'Observatoire de Grenoble, BP 53, 38041 Grenoble Cedex 9, France
- ⁷ Centro de Astrobiología (CSIC-INTA), Laboratorio de Astrofísica Molecular, Ctra. de Torrejón a Ajalvir, km 4, 28850 Torrejón de Ardoz, Madrid, Spain

- ⁸ Max-Planck-Institut für Radioastronomie, Auf dem Hügel 69, 53121 Bonn, Germany
- ⁹ LERMA, CNRS UMR8112, Observatoire de Paris and École Normale Supérieure, 24 rue Lhomond, 75231 Paris Cedex 05, France
- ¹⁰ LPMAA, UMR7092, Université Pierre et Marie Curie, Paris, France
- ¹¹ LUTH, UMR8102, Observatoire de Paris, Meudon, France
- ¹² I. Physikalisches Institut, Universität zu Köln, Zùlpicher Str. 77, 50937 Köln, Germany
- ¹³ Jet Propulsion Laboratory, Caltech, Pasadena, CA 91109, USA
- ¹⁴ Departments of Physics, Astronomy and Chemistry, Ohio State University, Columbus, OH 43210, USA
- ¹⁵ National Research Council Canada, Herzberg Institute of Astrophysics, 5071 West Saanich Road, Victoria, BC V9E 2E7, Canada
- ¹⁶ Infrared Processing and Analysis Center, California Institute of Technology, MS 100-22, Pasadena, CA 91125, USA
- ¹⁷ Canadian Institute for Theoretical Astrophysics, University of Toronto, 60 St George St, Toronto, ON M5S 3H8, Canada
- ¹⁸ Harvard-Smithsonian Center for Astrophysics, 60 Garden Street, Cambridge MA 02138, USA
- ¹⁹ National University of Ireland, Maynooth, Ireland
- ²⁰ SRON Netherlands Institute for Space Research, PO Box 800, 9700 AV, Groningen, The Netherlands
- ²¹ Department of Physics and Astronomy, University of Calgary, 2500 University Drive NW, Calgary, AB T2N 1N4, Canada
- ²² Department of Astronomy, University of Massachusetts, Amherst, MA, USA
- ²³ Université de Bordeaux, Laboratoire d'Astrophysique de Bordeaux, France; CNRS/INSU, UMR 5804, Floirac, France
- ²⁴ INAF - Istituto di Fisica dello Spazio Interplanetario, Roma, Italy
- ²⁵ Observatoire de Paris, LERMA UMR CNRS 8112, France
- ²⁶ School of Physics and Astronomy, University of Leeds, Leeds UK
- ²⁷ INAF Osservatorio Astrofisico di Arcetri, Florence, Italy
- ²⁸ Astronomical Institute "Anton Pannekoek", University of Amsterdam, Amsterdam, The Netherlands
- ²⁹ Department of Astrophysics/IMAPP, Radboud University Nijmegen, Nijmegen, The Netherlands
- ³⁰ IGN Observatorio Astronómico Nacional, Alcalá de Henares, Spain
- ³¹ INAF - Osservatorio Astronomico di Roma, Monte Porzio Catone, Italy
- ³² INAF - Istituto di Fisica dello Spazio Interplanetario, Roma, Italy
- ³³ Institut de RadioAstronomie Millimétrique, Grenoble, France
- ³⁴ Leiden Observatory, Leiden University, Leiden, The Netherlands
- ³⁵ Department of Physics and Astronomy, University College London, London, UK
- ³⁶ Department of Radio & Space Science, Chalmers University of Technology, Onsala, Sweden
- ³⁷ Institute of Astronomy, ETH-Zurich, Zurich, Switzerland
- ³⁸ Onsala Space Observatory, Chalmers Institute of Technology, Onsala, Sweden
- ³⁹ SETI Institute, Mountain View, CA, USA
- ⁴⁰ Department of Physics and Astronomy, San Jose State University, San Jose, CA, USA
- ⁴¹ Department of Astronomy, Stockholm University, Stockholm, Sweden
- ⁴² Observatoire de Paris, LUTH, and Université Denis Diderot, Meudon, France
- ⁴³ Stockholm Observatory, Stockholm, Sweden
- ⁴⁴ Institute Laboratoire d'Études du Rayonnement et de la Matière en Astrophysique, UMR 8112 CNRS/INSU, OP, ENS, UPMC, UCP, Paris, France and LERMA, Observatoire de Paris, Paris, France
- ⁴⁵ Max-Planck-Institut für Astronomie, Heidelberg, Germany
- ⁴⁶ Kapteyn Astronomical Institute, University of Groningen, The Netherlands